Reprinted from

Journal of Electron Spectroscopy and Related Phenomena

Journal of Electron Spectroscopy and Related Phenomena, 68 (1994) 605–616

Effects of Elastic and Inelastic Electron Scattering on Quantitative Surface Analyses by AES and XPS

C. J. Powell,[a] A. Jablonski,[b] S. Tanuma,[c] and D. R. Penn[a]

[a]National Institute of Standards and Technology, Gaithersburg, MD 20899, USA

[b]Institute of Physical Chemistry, Polish Academy of Sciences, ul. Kasprzaka 44/52, 01-224 Warsaw, Poland

[c]Analysis Research Center, Nippon Mining Company, Ltd., 3-17-35 Niizo-Minami, Toda, Saitama 335, Japan

ELSEVIER

Journal of Electron Spectroscopy and Related Phenomena, 68 (1994) 605–616

Effects of Elastic and Inelastic Electron Scattering on Quantitative Surface Analyses by AES and XPS

C. J. Powell,[a] A. Jablonski,[b] S. Tanuma,[c] and D. R. Penn[a]

[a]National Institute of Standards and Technology, Gaithersburg, MD 20899, USA

[b]Institute of Physical Chemistry, Polish Academy of Sciences, ul. Kasprzaka 44/52, 01-224 Warsaw, Poland

[c]Analysis Research Center, Nippon Mining Company, Ltd., 3-17-35 Niizo-Minami, Toda, Saitama 335, Japan

A review is given that describes the complications due to elastic and inelastic electron scattering in quantitative surface analyses by Auger-electron spectroscopy and x-ray photoelectron spectroscopy. Four principal topics are addressed. First, the simple formulae for surface analyses are based on a model that ignores elastic scattering. Recent work assessing the effects of elastic scattering is summarized which shows that the simple formulae are valid in certain analytical situations but with an appropriate choice of the parameter describing inelastic scattering. Second, we review measurements of effective attenuation lengths and point out many sources of significant systematic error in these measurements. Third, we describe recent calculations of inelastic mean free paths (IMFPs) in over fifty materials that have been utilized to develop a predictive IMFP formula. Finally, we discuss the complicating effects of inelastic scattering on reliable measurements of AES and XPS intensities.

1. INTRODUCTION

It has long been recognized that the surface sensitivity of Auger-electron spectroscopy (AES) and x-ray photoelectron spectroscopy (XPS) measurements is due to the very strong inelastic scattering of electrons in the 50-2000 eV range of practical interest [1-4]. For this energy range, the electron inelastic mean free paths (IMFPs) are typically in the range 3-100 Å for many materials. Surface sensitivity for a particular material and electron energy can be enhanced by the use of near-grazing takeoff angles, the use of near-grazing beams of incident x-rays [5], or by the use of coincidence techniques [6].

The effects of elastic electron scattering in AES and XPS, however, have not been as widely appreciated as those of inelastic scattering. In an important series of papers, Baschenko and Nefedov [7] showed that elastic electron scattering modified the angular and depth distributions of the signal electrons in XPS. Further investigations of elastic electron scattering effects in quantitative AES and XPS have now been reported by other authors [8-21]. As a result of elastic scattering, the intensity of signal electrons from a substrate may not vary exponentially with the thickness of an overlayer film. In addition, the IMFP for a given material and electron energy will be systematically larger (by up to 40%) than the corresponding effective attenuation lengths (EALs) (for situations where the attenuation of signal electron is approximately exponential with distance from the surface). The actual difference between the IMFP and the EAL will depend, in general, on electron energy, the atomic number(s) of the element(s) involved, and the experimental configuration.

Quantitative surface analyses by AES and XPS are now based on formulae obtained from a model in which the effects of elastic electron scattering were assumed to be neglible. In this paper, we will first summarize results which show that the formulae in common use can be applied to some analytical situations but only with an appropriate choice of the parameter describing inelastic scattering. We will then discuss the measurement of EALs and

SSDI 0368-2048(94)02164-U

distribution of the signal electrons, however, is not significantly affected by elastic collisions [10,13]. It was therefore convenient to define a correction parameter Q

$$Q = I^{el}/I^{nel} \quad (2)$$

Monte Carlo simulations for the geometry of the cylindrical mirror analyzer (CMA), as well as for other analyzers operated with the same electron emission angle, showed that the DDF is close to exponential [10,13]. The DDF could then be expressed as

$$\phi_{\alpha}^{el}(z) = \exp(-z/L\cos\alpha)/L\cos\alpha \quad (3)$$

where L is the effective attenuation length (EAL) determined from the Monte Carlo simulations. The corresponding expression for the situation when elastic scattering is ignored is

$$\phi_{\alpha}^{nel}(z) = \exp(-z/\lambda\cos\alpha)/\lambda\cos\alpha \quad (4)$$

where λ is the electron inelastic mean free path. For the case of an exponential DDF, it was convenient to introduce a second correction parameter K given by

$$K = L/\lambda \quad (5)$$

The value of K depends on the experimental configuration (emission angle, solid angle of analyzer), the Auger-electron transition, and the matrix; for some conditions, K can be as small as 0.7.

We consider now three analytical applications in AES. The first application is the analysis of a surface volume which is homogenous over the sampling depth of the AES measurement. From Eq. (2), we obtain $I^{el} = QI^{nel} \propto Q\lambda$. Thus, the total signal current is found to be proportional to the product $Q\lambda$. Proportionality only to λ would be expected if the elastic collisions are neglected. Since the correction factor Q is close to unity, little error is introduced if this factor is ingnored. Thus, the IMFP rather than the EAL should be utilized in determination of the surface composition. This conclusion is valid irrespective of the shape of the DDF.

Second, we consider a measurement of the thickness of a thin film on a substrate. The equations for the signal currents from the film and the substrate indicate that the film thickness is related to the EAL (=Kλ) for situations where the DDF is exponential; if the DDF is non-exponential, the particular expression for the DDF has to be used in place of Eq. (3). The equations for the signal currents are also valid only when the film and substrate have similar elastic scattering properties. Monte Carlo calculations for a wide range of conditions, however, have shown that the signal currents depend weakly on the substrate atomic number [12,34].

The final application concerns determination of the average depth of analysis. The mean escape depth D for the signal electrons is given by

$$D = \int_0^{\infty} z\,\phi_{\alpha}^{el}(z)\,dz \quad (6)$$

If the DDF is exponential, then $D = L\cos\alpha$.

A similar analysis can be made for XPS although the situation is more complicated on account of the angular anisotropy of the photoemission [32]. The differential photoionization cross section can be expressed in the form

$$d\sigma_x/d\Omega = \sigma_x\, W(\psi,\beta) \quad (7)$$

where σ_x is the total photoionization cross section, $W(\psi,\beta)$ describes the angular anisotropy, ψ is the angle between the direction of the x-rays and the direction of analysis, and β is the asymmetry parameter [35]. The term $W(\psi,\beta)$ is given by

$$W(\psi,\beta) = [1-(\beta/4)(3\cos^2\psi - 1)]/4\pi \quad (8)$$

We assume that the specimen is irradiated by a broad beam of x-rays and that the specimen area viewed by the analyzer varies inversely as $\cos\alpha$.

Monte Carlo simulations show that the XPS signal current I^{el} may be either smaller or larger than

of different types of film growth by Argile and Rhead [40]. Seah [41] in 1972 evaluated the effects of statistical thickness non-uniformities on the rate of decay of substrate signal intensity and found non-exponential decays. It was then reasonable in subsequent work for non-exponential decays to be discarded on account of the presumed insufficiently uniform film growth. Monte Carlo simulations of the overlayer-film experiment, however, have indicated that non-exponential decays are to be expected for some measurement situations, even when a uniform overlayer is assumed [12]. This result is related to the possibly non-exponential behavior of the DDF. It is now clear from measurements made with scanning tunneling microscopy and low-energy electron microscopy that film growth in the early stages (<5 monolayers) can be extremely complex. Yet another problem is the possible intermixing of the substrate and film in the vicinity of the interface. Since the minimum value of the EAL in many materials is about 3 Å, it is clear that the morphology and structure of deposited films has to be determined on an atomic scale if reliable measurements are to be made of the EAL when this is less than about 10 Å.

Second, the EAL is commonly regarded as a "bulk" quantity, independent of film thickness. The excitation of surface plasmons at the surfaces of free-electron-like materials, however, could make the EAL dependent on film thickness [42]. The strength of interferences between intrinsic plasmon excitation (e.g., caused by shakeup in the photoionization process) and extrinsic plasmon excitation (e.g., caused by inelastic scattering of a photoelectron) can also depend on overlayer film thickness [43]. In addition, EAL measurements may be affected by possible atomic reconstructions at both the film surface and the substrate-film interface.

Finally, no account has been taken of the potentially strong angular anisotropies in electron transport due to elastic scattering in crystalline solids [27,28]. In one striking experiment by Egelhoff [44], a 1.5 monolayer film of Cu overlaying a 0.3 monolayer Ni film caused nearly a factor of two increase (rather than an exponential decrease) of the Ni XPS signal. These effects are due to the strong forward-focusing effects referred to above in rows of atoms and are particularly strong in epitaxial films deposited on single-crystal substrates [27,28].

It is very difficult to estimate the possible magnitudes of the effects listed above in reports of EAL measurements. One indication of the general likelihood of substantial systematic uncertainties in many measurements lies in the frequently large variations in EAL data for a given material and energy. It is not uncommon to find variations of a factor of two or more in reported EAL values for supposedly the same material and energy [39].

In retrospect, it is at first sight difficult to understand why many experimentalists reported exponential or near-exponential dependences of AES or XPS intensity on overlayer film thickness (for non-crystalline solids) when it is now known that elastic scattering effects could be expected to have led to noticeable deviations from exponential dependences. The reason for the lack of a significant number of reports of deviations from exponential dependences of AES and XPS intensities on film thickness is believed to be due to the fact that most experimentalists expected to observe exponential dependences and had good reason to discard contrary data as being associated with film nonuniformities [41]. Although the early stages of film growth have been investigated for many years, the many complexities in film nucleation and growth have been recognized only recently with the advent of more sensitive structural probes [40].

In 1979, Seah and Dench [4] published a review of EAL data in which they analyzed the possible dependences of EAL values on different material parameters. They found least scatter about a common curve when the effective attenuation length L was expressed as

(a) for elements

$$L = 538\, aE^{-2} + 0.41a^{3/2} E^{1/2} \text{ nm} \qquad (9a)$$

(b) for inorganic compounds

$$L = 2170\, aE^{-2} + 0.72a^{3/2} E^{1/2} \text{ nm} \qquad (9b)$$

for each material. Since the optical data used in the IMFP calculations for the elements and for the organic compounds were generally superior to the optical data for the compounds (as judged by the sum-rule tests), the set of values of the four parameters for each of the 27 elements and the 14 organic compounds was analyzed in terms of various material parameters to yield the following empirical relationships [55]

$$\beta = -0.10 + 0.944/(E_p^2 + E_g^2)^{1/2} + 0.069\rho^{0.1} \quad (12a)$$

$$\gamma = 0.191\ \rho^{-0.50} \quad (12b)$$

$$C = 1.97 - 0.91\ U \quad (12c)$$

$$D = 53.4 - 20.8\ U \quad (12d)$$

$$U = N_v\rho/M = E_p^2/829.4 \quad (12e)$$

where E_g is the bandgap energy (in eV) for non-conductors. Equations (11) and (12) were found to give IMFP values that differed by 10% RMS (root-mean-square) from those calculated directly from the optical data for the elements and by about 9% for the organic compounds. As a result, Eqs. (11) and (12) constitute a useful predictive equation (designated TPP-2M) for estimating IMFPs in other materials.

An earlier analysis based on the IMFP data for the group of 27 elements alone yielded a different expression for the parameter β than that shown in Eq. (12a) [51]

$$\beta = -0.0216 + 0.944/(E_p^2 + E_g^2)^{1/2} + 7.39 \times 10^{-4}\rho \quad (13)$$

This analysis (which yielded the predictive IMFP formula designated TPP-2) was based on materials with relatively high densities (predominantly transition metals).

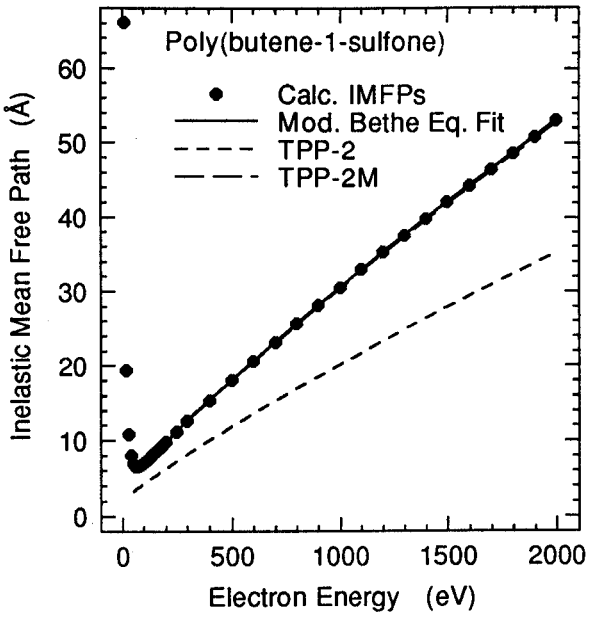

Figure 1. IMFP values (solid circles) calculated for poly(butene-1-sulfone) as a function of electron energy [55]. The solid line is a fit to the IMFP values with the modified Bethe equation [Eq. (11)]. The long-dashed line (nearly coincident with the solid line) shows IMFP values from the predictive formula TPP-2M [Eqs. (11) and (12)] while the short-dashed line shows IMFP values from the TPP-2 formula [Eq. (13) used instead of Eq. (12a) for the parameter β in Eq. (11)].

Figure 1 shows an example of the IMFP results for poly(butene-1-sulfone), a resist material used for ion- and electron-beam lithography [58]. The solid line is a fit of Eq. (11) to the calculated IMFPs in which the four parameters β, γ, C and D were allowed to vary [55]. The long-dashed line (almost coincident with the solid line) is a plot of TPP-2M while the short-dashed line is a plot of TPP-2. From this and similar comparisons with the other materials in the group of organic compounds [55], it was concluded that the TPP-2M predictive formula was superior to the TPP-2 formula; for the group of elements, both formulae gave generally satisfactory results.

We note here that there are differences in technical approach among the several recent efforts to calculate IMFPs [49-55,59-61]. For electron energies between 200 and 2000 eV, the results from the different groups for the same material differ by up to 11%, but larger differences, up to about 50%, occur between 50 and 200 eV. The latter differences are associated with different approaches for treating exchange and correlation effects; there is currently no consensus on how to include these effects in the IMFP calculation.

The IMFP calculations described briefly here are for bulk solids. It would be expected that modifications to the IMFPs should occur in the vicinity of surfaces (e.g., due to the excitation of surface plasmons in free-electron-like solids) [54]. Yubero and Tougaard [62] recently showed that the effective IMFP could change with path-length for reflection electron energy-loss spectroscopy on the basis of two models for the electron-surface interaction. Further comments on uncertainties in the IMFP calculations are presented elsewhere [54].

The IMFP can be determined from measurements of the elastic electron backscattering probability from surfaces [63]. This type of measurement depends on knowledge of the differential elastic scattering cross sections for all elemental constituents of the solid; these cross sections are currently obtained from theory. Experiments can be performed with any type of analyzer, e.g., a retarding-field analyzer of the type used for low-energy electron diffraction experiments or a cylindrical-mirror analyzer. The advantage of this technique for measuring IMFPs is that experiments can be performed with macroscopic specimens rather than the thin overlayer films needed for EAL measurements. The relatively few published IMFP measurements agree reasonably well with calculated IMFPs [63] although, in some instances, the measured IMFPs vary more rapidly with electron energy than expected from the calculations; the reason for such deviations is not known. Sources of possible uncertainty in this type of IMFP measurement are discussed elsewhere [32].

5. INTENSITY MEASUREMENTS

The AES or XPS signal of interest for a given element may consist of a single peak, a set of peaks at energies characteristic of the element, or one or more groups of peaks at characteristic energies with each group containing two or more peaks associated with different physical or chemical states of that element. Other reviews contain a discussion of factors important for determining the relative peak intensities of different elements in the particular analysis [39,64].

We give some brief remarks here on intensity measurement for the simple situation when a single AES or XPS peak is observed. In the so-called direct mode of spectrum measurement [39], it is common to separate the intensity of the peak of interest from the background intensity due to secondary electrons, to scattered primary electrons (AES) or photoelectrons (XPS), and to photoelectrons excited by bremsstrahlung (XPS). This background has been termed the matrix background [39] since it refers to the background for some matrix if the AES or XPS signal from the element of interest was absent. The AES or XPS signal from the selected element can be considered to be of two parts, a part due to Auger electrons or photoelectrons that have not been inelastically scattered in the specimen material and a part due to such electrons that have been inelastically scattered. The first part is the intensity that should be measured in a quantitative analysis. This component contains not only the intensity of the "main" peak but also a continuous intensity and features that are each due to intrinsic excitations accompanying core-electron excitation or decay. The intensity associated with the intrinsic excitation is frequently ignored in quantitative AES or XPS even though there are instances where the fraction of intensity due to intrinsic processes relative to the main peak changes drastically with chemical state. Although the intrinsic component of the spectrum may frequently not be obvious (in structure or intensity), it is generally not neglible [39,64]. The practical problem here is the separation of the overlapping intensities due to intrinsic excitations and inelastic scattering.

14. Z.-J. Ding, Ph.D. Thesis, Osaka University (1990).
15. W.S.M. Werner, W.H. Gries and H. Stori, J. Vac. Sci. Tech. A, 9 (1991) 21.
16. W.S.M. Werner, W.H. Gries and H. Stori, Surf. Interface Anal., 17 (1991) 693.
17. Y.F. Chen, C.M. Kwei and C.J. Tung, J. Phys. D., 25 (1992) 262.
18. W.S.M. Werner, Surf. Interface Anal., 18 (1992) 217; W.S.M. Werner, J. Electron Spectrosc. Relat. Phenom., 59 (1992) 275.
19. I.S. Tilinin and W.S.M. Werner, Phys. Rev. B, 46 (1992) 13739; W.S.M. Werner and I.S. Tilinin, Appl. Surf. Sci., 70/71 (1993) 29.
20. P.F.A. Alkemade, K. Werner, S. Radelaar and W.G. Sloof, Appl. Surf. Sci., 70/71 (1993) 24.
21. P.J. Cumpson, Surf. Interface Anal., (in press).22. H.E. Bishop and J.C. Riviere, J. Appl. Phys., 40 (1969) 1740.
23. B.L. Henke, Phys. Rev. A, 6 (1972) 94.
24. P.W. Palmberg, Anal. Chem., 45 (1973) 549A.
25. C.S. Fadley, in G. Somorjai and J. McCaldin (eds.), Progress in Solid State Chemistry, Pergamon Press, New York, 1976, p. 265.
26. C.J. Powell, in N.S. McIntyre (ed.), Quantitative Surface Analysis of Materials, ASTM Special Technical Publication 643, American Society for Testing and Materials, Philadelphia, 1978, p. 5.
27. S.A. Chambers, Surf. Sci. Reports, 16 (1992) 261.
28. W.F. Egelhoff, Jr., in J.A.C. Bland and B. Heinrich (eds.), Ultrathin Magnetic Structures, Springer-Verlag, New York, 1993 (in press).
29. W.H. Gries, Surf. Interface Anal., 17 (1991) 803.
30. H.E. Bishop, B. Chornik, C. LeGressus and A. Le Moel, Surf. Interface Anal., 6 (1984) 116; F.E. Doern, L. Kover and N.S. McIntyre, Surf. Interface Anal., 6 (1984) 282; P. Morin, Surf. Sci., 164 (1985) 127.
31. H.E. Bishop, Surf. Interface Anal., 15 (1990) 27; H.E. Bishop, Surf. Interface Anal., 17 (1991) 197.
32. A. Jablonski and C.J. Powell, Surf. Interface Anal., 20 (1993) 771.
33. P. Maciejewski, U. Höfer, W. Wurth and E. Umbach, J. Electron Spectrosc. Relat. Phenom., 62 (1993) 1.
34. W.S.M. Werner, Surf. Sci., 257 (1991) 319.
35. R.F. Reilman, A. Msezane, and S.T. Manson, J. Electron Spectrosc. Relat. Phenom., 8 (1976) 389.
36. A. Jablonski, M.F. Ebel and H. Ebel, J. Electron Spectrosc. Relat. Phenom., 40 (1986) 125.
37. C.J. Powell, Scanning Electron Microsc., 4 (1984) 1649.
38. C.J. Powell, J. Electron Spectrosc. Relat. Phenom., 47 (1988) 197.
39. C.J. Powell and M.P. Seah, J. Vac. Sci. Technol. A, 8 (1990) 735.
40. C. Argile and G.E. Rhead, Surf. Sci. Reports, 10 (1989) 277.
41. M.P. Seah, Surf. Sci. 32 (1972) 703.
42. P.J. Feibelman, Surf. Sci., 36 (1973) 558; M. Sunjic and D. Sokcevic, Sol. State Comm., 15 (1974) 165.
43. M. Sunjic, D. Sokcevic and J.W. Gadzuk, Jpn. J. Appl. Phys. Suppl., 2 (2) (1974) 753; D. Sokcevic and M. Sunjic, Sol. State Comm., 15 (1974) 1703; D. Sokcevic and M. Sunjic, Phys. Rev. B., 30 (1984) 6965.
44. W.F. Egelhoff, Jr., Phys. Rev. B, 30 (1984) 1052; Phys. Rev. Letters, 59 (1987) 559.
45. C.D. Wagner, L.E. Davis and W.M. Riggs, Surf. Interface Anal., 2 (1980) 53; H. Ebel, M.F. Ebel, P. Baldauf and A. Jablonski, Surf. Interface Anal. 12 (1988) 172.
46. H. Bethe, Ann. Physik, 5 (1930) 325.
47. C.J. Powell, Surf. Interface Anal., 7 (1985) 256.
48. C.J. Powell, R.J. Stein, P.B. Needham, Jr., and T.J. Driscoll, Phys. Rev. B, 16 (1977) 1370.
49. D.R. Penn, Phys. Rev. B, 35 (1987) 482.
50. S. Tanuma, C.J. Powell, and D.R. Penn, Surf. Interface Anal., 11 (1988) 577.
51. S. Tanuma, C.J. Powell, and D.R. Penn, Surf. Interface Anal., 17 (1991) 911.
52. S. Tanuma, C.J. Powell, and D.R. Penn, Surf. Interface Anal., 17 (1991) 927.
53. S. Tanuma, C.J. Powell, and D.R. Penn, Acta Physica Polonica A, 81 (1992) 169.
54. S. Tanuma, C.J. Powell, and D.R. Penn, Surf. Interface Anal., 20 (1993) 77.
55. S. Tanuma, C.J. Powell, and D.R. Penn, (to be published).
56. J. Lindhard and M. Scharff, K. Dan. Vidensk. Mat.-Fys, Medd., 27 (1953) No. 15; J. Lindhard, M. Scharff, and H.E. Schiott, K. Dan. Vidensk. Mat.-Fys. Medd. 33 (1963) No. 14; D. Pines,